Magnetic Hardening of Rapidly Solidified $SmFe_{7+x}M_x$ (M=Mo, V, Ti) Compounds

Choong Jin Yang, E. B. Park and S. D. Choi
Electromagnetic Materials Laboratory, Research Institute of
Industrial Science & Technology(RIST), Pohang 790-600, Korea

(Received 12 June 1994, in final form 13 Setpember 1994)

Rapidly solidified $SmFe_{7+x}M_x$ (M = Mo, V, Ti) compound were found to crystallize in the $Sm(Fe, M)_7$ based stable magnetic phase by introducing a second transition element into the Sm-Fe binary system. The $Sm(Fe, M)_7$ phase exhibits the highest Curie temperature(T_c = 355 ℃) ever known in the Sm-Fe magnetic systems with a quite high intrinsic coercivity($_iH_c$ = 3 ~ 6 kOe). The $Sm(Fe, M)_7$ phase remains stable even after annealing if once form during the rapid solidification. The primary reason for the high coercive force is due to the fine grain size(2000 ~ 8000 Å) of the magnetic $Sm(Fe, M)_7$ matrix phase, and the enhanced Curie temperature is attributed to the extended solid-solubility of the additive transition elements in Fe matrix, which leads to volume expansion of the $Sm(Fe, M)_7$ cell causing an enhanced coupling constant of Fe atoms.

Ⅰ. Introduction

Following the discovery of the $Nd_2Fe_{14}B$ based compound, extensive investigations have been focussed on the $ThMn_{12}$ based compounds. By alloying small amounts of a third element M(M = Ti, V, Cr, Mo, Si) to Sm-Fe(Fe-rich) systems, a number of new phases with interesting hard magnetic properties were reported to form[1-3]. Like the $Nd_2Fe_{14}B$ phase, the tetragonal $Sm(Fe, M)_{12}$ structure shows promising characteristics such as strong uniaxial anisotropy[1-2] and a Curie temperature of 310 ℃ as well as a high saturation magnetization[3]. Besides the 1 : 12 phase, an extremely hard magnetic Sm_2Fe_7Ti type compound (called A_2 which was firstly named by Schneider et al.[4] in the Nd-Fe system) was observed in sputtered thin films[5], and subsequently in mechanically alloyed[6] and melt-spun ribbons[7] by Katter et al. Recently, Stadelmaier et al.[8] gave a comparison of the X-ray indexing of the Sm-Fe-Ti(A_2 phase), and identified the A_2 phase as Sm_5Fe_{17}. A complete indexing of the high coercive A_2 phase based on a hexagonal cell(a = 20.12, c = 12.34 Å) was reported by Cadieu et al.[9]. However, the studies of Ref. 8 and 9 remain arguable due to the ambiguous conclusion whether the M element is be in some grain boundary phases or in the matrix magnetic phase.

During the course of efforts to prepare $SmFe_{7+x}M_x$(M = Mo, V, Ti) single phased materials, we found that a new class of compound having the $Sm(Fe, M)_7$ stoichiometry exhibits hard magnetic properties. In this study we report the magnetic properties and microstructural identification of the $Sm(Fe, M)_7$ phase.

Ⅱ. Experimental

Using elemental Sm(purity 99.5 %), Fe(99.99 %) and M(M = Mo, Ti and V, 99.9 %), the $SmFe_{7+x}M_x$ precursors were melted by induction heating under an Ar gas atmosphere. The precursors, of which the x varies from 0.2 to 2.0 with a compositional interval 0.2 at.%, were then remelted for three times to be homogeneous. Weight loss during the melting caused by Sm evaporation was compensated by adding excess 1 % Sm respective to the total weight of each precursor. Rapidly quenched ribbons were pepared by

melt-spinning onto a conventional copper wheel rotating at a line speed of 30 m/sec. Annealing at 650 ~ 750 ℃ was carried out by sealing the samples into an argon gas filled quartz tube. X-ray diffraction analysis was performed with a Rigaku's XRD-MXC diffractometer using Cu Kα radiation. Magnetic properties of the ribbon samples were measured at room temperature using a vibrating sample magnetometer(Toei's VSM-5) under a magnetic field of 16 kOe. In every measurements appropriate demagnetization factor was taken in account based on the sample geometry. Thermomagnetic curves were obtained using a Perkin-Elmer analyzer(TGA-7) in a magnetic field of 30 Oe. Microstructural phase identification was carried out by electron microscopy(SEM, TEM) and microanalysis techniques(EPMA, EDX) in addition to the X-ray diffractometry.

Ⅲ. Results and Discussion

3. 1. Magnetic properties

In Fig. 1 and 2, the typical magnetic properties of the melt-spun $SmFe_{7+x}M_x$ (M = Mo, V, Ti) compounds are shown as a function of the addition of M elements. Fig. 1 denotes the properties measured from the as-spun ribbons, and Fig. 2 is for

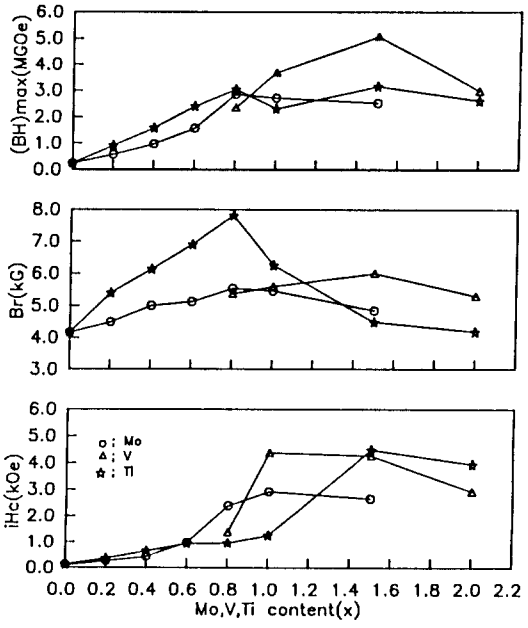

Fig. 1. Magnetic properties of melt-spun $SmFe_{7+x}M_x$ (M = Mo, V, Ti) ribbons as a function of M addition before heat treatment(measured in plane direction)

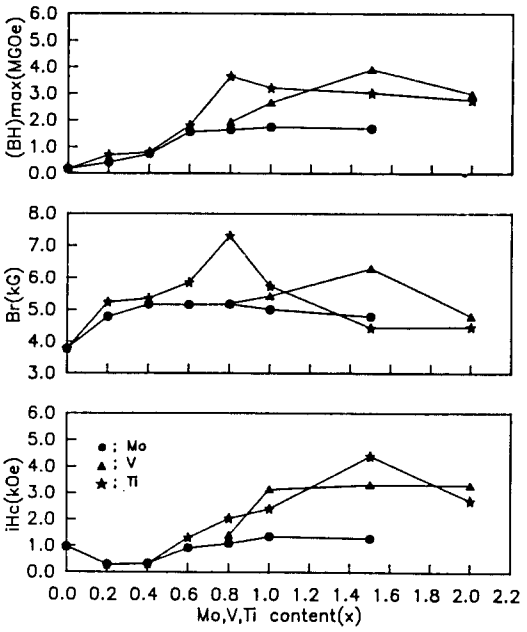

Fig. 2. Magnetic properties of melt-spun $SmFe_{7+x}M_x$ (M = Mo, V, Ti) ribbons as a function of M addition after heat treatment(measured in plane direction)

the annealed samples at 700 ℃ for one hour. Since the magnetic properties obtained both in-plane direction and in the perpendicular direction to the ribbon surface showed almost identical trends and slightly higher values, the properties from the in-plane direction are only discussed. Basically, the principal magnetic properties($_iH_c$, B_r and $(B.\ H)_{max}$) of the melt-spun compounds increase with the addition of Mo, V and Ti up to a certain composition x, and then decline thereafter. However, the composition x giving the maximum value in each $_iH_c$, B_r and $(B.\ H)_{max}$ is not the same for the pseudo-binary compound of different additive. For the $SmFe_{7+x}M_x$ the $_iH_c$, B_r and $(B.\ H)_{max}$ are maxmized simultaneously at x = 0.8 ~ 1.0 and then tend to decrease thereafter. For the $SmFe_{7+x}V_x$ and $SmFe_{7+x}Ti_x$ samples, however, the coercivity

values increase monotonically up to x = 1.5 giving a $_iH_c$ of 5 kOe, and then decline thereafter. The resultant energy product, $(B.H)_{max}$, obtained from the $SmFe_{8.5}V_{1.5}$ and $SmFe_{8.5}Ti_{1.5}$ compounds were 5.0 MGOe and 3.4 MGOe, respectively. Particularly, the $SmFe_{7+x}Ti_x$ compounds exhibited considerably high remanence(B_r) vales of 6 to 8 kG between x = 0.4 and 1.0. However, since the coercivity values are rather low in this range, the energy product of 3.2 MGOe is obtained from the $SmFe_{7.8}Ti_{0.8}$ composition. After annealing the $SmFe_{7.8}Mo_{0.8}$ the maximum energy product of 3.0 MGOe was obtained, while the $SmFe_{8.5}V_{1.5}$ and $SmFe_{7.8}Ti_{0.8}$ compounds show the $(B.H)_{max}$ of 4.0 MGOe in Fig. 2.

Curie temperature of the Sm-Fe binary systems was considerably enhanced by introducing Mo, V and Ti to form $SmFe_{7+x}M_x$ ternary systems. Fig. 3

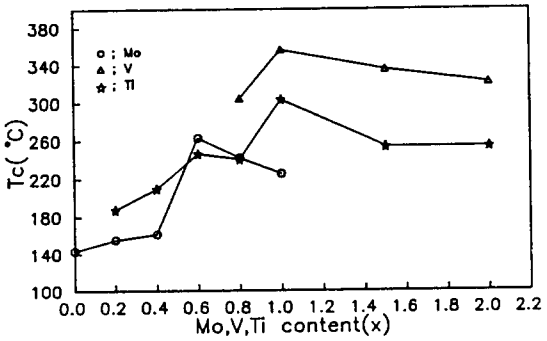

Fig. 3. Varation of Curie temperature of melt-spun $SmFe_{7+x}M_x$(M = Mo, V, Ti) ribbons as a function of M addition.

shows the variation of Curie temperature of the melt-spun $SmFe_{7+x}M_x$. The Curie temperature increases as a function of M addition up to a certain composition x, and then decreases with the further addition of M. A Curie temperature of 270 ℃ was obtained at x = 0.6 for the $SmFe_{7.6}Mo_{0.6}$, while 300 ℃ and 355 ℃ were achieved at x = 1.0 for the $SmFe_8Ti$ and $SmFe_8V$ compounds, respectively. These levels of Curie temperature are quite high compared with those from the previously known $SmFe_{12}$[1-3] or Sm_5Fe_{17}[8] based structures. In the mean-molecular-field model the Curie temperature of the various rare-earth iron compounds can be expressed as

$$3kT_c = \alpha_{FeFe} + (\alpha^2_{FeFe} + 4\,\alpha_{RFe}\alpha_{FeR})^{1/2}$$

where the magnetic interaction energy between the R atoms (α_{RR}) is neglected, then

$$\alpha_{FeFe} = Z_{FeFe}J_{FeFe}S_{Fe}(S_{Fe}+1),$$
$$\alpha_{RFe}\alpha_{FeR} = Z_{RFe}Z_{FeR}S_{Fe}(S_{Fe}+1)(g_J-1)J(J+1)J^2_{RFe}$$

where all the terminologies are defined elsewhere [10]. According to this model the Curie temperature is mostly influenced by the exchange energy between the Fe atoms(α_{FeFe}), therefore by both the everage number of Fe neighbor atoms to Fe (Z_{FeFe}) as well as the coupling constant(J_{FeFe}). The coupling between the R and Fe atoms would be smaller. In this regard, taking into account the atomic radius(or ionic radius) of each additive Mo, V and Ti elements, the expected T_c for the $SmFe_{7+x}M_x$(M = V, Mo, Ti) at a certain x must be either in order of V > Mo > Ti or Ti > Mo > V when only the Z_{FeFe}(or Z_{RFe}, Z_{FeR}) is concerned. Because the atomic radius of each V, Mo and Ti is 1.32, 1.36 and 1.47 Å, respectively. However, this was not true as shown in Fig. 3 where the $SmFe_{7+x}V_x$ compound always exhibit the highest T_c over the entire x range. Accordingly, not only the Z_{FeFe} (or Z_{RFe}, Z_{FeR}) but the J_{FeFe}(or J_{RFe}) would also change at the same time in the way that the replacement of M atoms for Fe leads to volume expansion of the Sm(Fe, M)$_7$ cell causing an enhanced J_{FeFe}(or J_{RFe})[9].

3. 2. Identification of magnetic phase

Considering the magnetic transformation taking place through the variation of M addition in the $SmFe_{7+x}M_x$ shown in Figs. 1 and 2, the existing magnetic phase(or phases) was identified by choosing the $SmFe_{7.8}M_{0.8}$ and $SmFe_8M$ stoichiometries which exhibit the excellent magnetic proper-

ties. First of all, rapidly quenched precursor of $SmFe_7$ stoichiometry was prepared and characterized by indexing the reflected peaks. The $SmFe_7$ precursor crystallized mostly in the $TbCu_7$ type 1 : 7 stoichiometry[11-12] with a certain amount of Sm_2Fe_{17} crystals represented by the well-resolved(204) and (211) reflections from the rhombohedral structure. No free α-Fe was observed in this $SmFe_7$ precursor. However, when a Fe-riched $SmFe_5$ precursor was rapidly quenched by the same condition, the $SmFe_7$ crystallization was observed be accompanied by $SmFe_2$ phase as shown in Fig. 4.

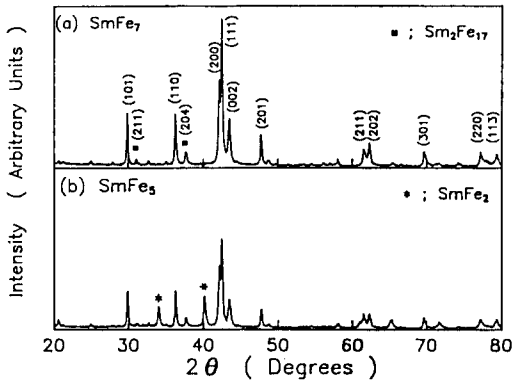

Fig. 4. X-ray diffraction patterns of as-spun (a) Sm Fe_7 and (b) $SmFe_5$ ribbons, respectively.

Unlike the binary $SmFe_5$ or $SmFe_7$, the addition of M elements into the binary system leads to the formation of some amount of Fe_3M and α-Fe which are magnetically soft. Instead $Sm_2(Fe, M)_{17}$ and $SmFe_2$ phases tend to disappear suggesting that the $Sm(Fe, M)_7$ phase becomes stable by introducing the second transition elements(Mo, V and Ti) into the $SmFe_7$ structure. This fact was true for all the as-spun $SmFe_8M$(M = Mo, V, Ti) ribbons. It is very plausible to consider the coupling force that the substituionally solutionized second transition M atoms would have more attractive coupling force with Fe atoms than the Sm atoms do with Fe. This idea was already assumed in the previous chapter discussing the mean-molecular-field model. Fig. 5 shows X-ray diffraction pattern

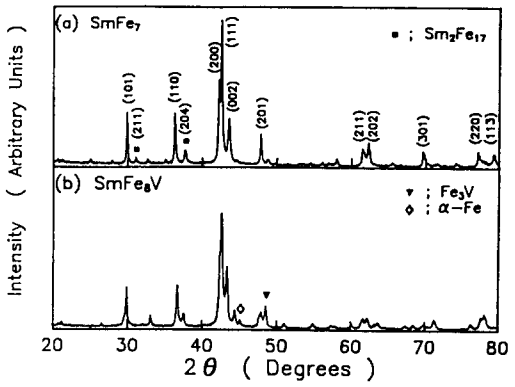

Fig. 5. X-ray diffraction patterns of as-spun (a) Sm Fe_7 and (b) $SmFe_8$ ribbons, respectively.

of the typical $SmFe_8V$ compound. It is obvious in Fig. 5(b) that the addition of V into the $SmFe_7$ system make the $Sm(Fe, V)_7$ phase stable. Only the presence of Fe_3V and α-Fe are indicated though neglegible. Besides, the stablized $Sm(Fe, M)_7$ phase was found not to be changed even after annealing at 600 ~ 750 ℃ for 1 ~ 2 hours. This should be a merit of this compound for the use of resin bonded magnets. Fig. 6 and 7 shows the

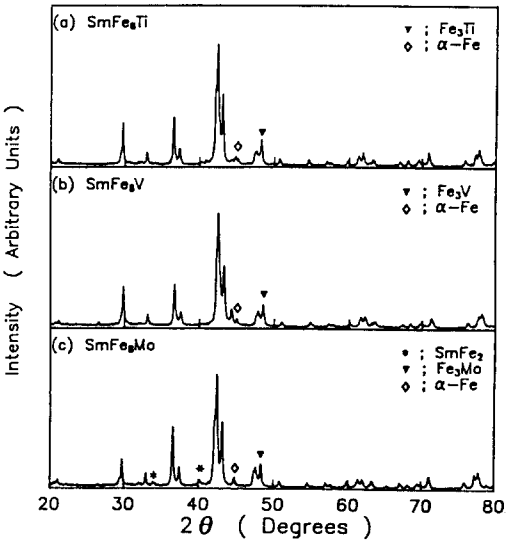

Fig. 6. X-ray diffraction patterns of as-spun (a) Sm Fe_8Ti, (b) $SmFe_8V$ and (c) $SmFe_8Mo$ ribbons, respectively.

한국자기학회지 Volume 4, Number 3, September 1994

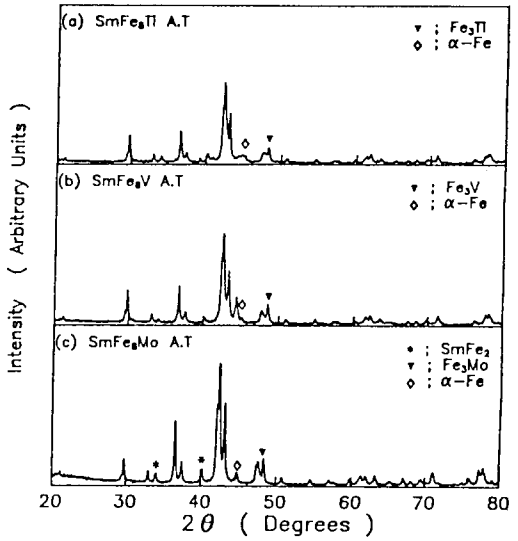

Fig. 7. X-ray diffraction patterns of melt-spun (a) $SmFe_8Ti$, (b) $SmFe_8V$ and (c) $SmFe_8Mo$ ribbons, respectively.

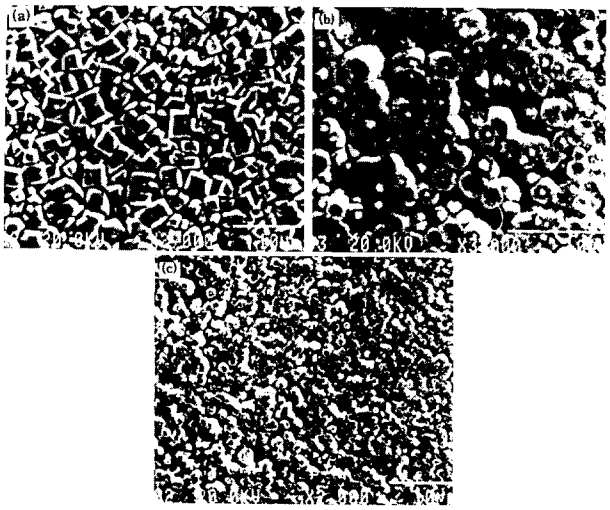

Fig. 8. SEM micrographs showing the $Sm(Fe, M)_7$ crystals at the surface of (a) $SmFe_8Mo$, (b) $SmFe_8V$ and (c) $SmFe_8Ti$ ribbons, respectively.

X-ray diffraction patterns of $SmFe_8M$(M = Mo, V, Ti) compounds before and after annealing. Only some amount of $SmFe_2$ in addition to Fe_3Mo and α-Fe is indicated in the $SmFe_8Mo$ compound. It is of worth to note that the authors have already reported the formation of $NdFe_7$ phase in melt-spun $NdFe_2$ compound[13-14]. The metastable $NdFe_7$(rhombohedral system in hexagonal axes) phase was found to be embedded in Nd-rich matrix which exhibits a high coercivity($_iH_c$ = 2 ~ 3.5 kOe) and Curie temperature(T_c = 230 ~ 235 ℃) as well. After annealing, however, the magnetically hard $NdFe_7$ phase was transformed into Nd_2Fe_{17} plus Nd_5Fe_{17} which showed very low coercivity value ($_iH_c$ = 0.18 kOe) although the Curie temperature was not changed.

The single phased $SmFe_8M$ grains are well developed in the as-spun ribbon's surface as shown in Fig. 8(a), (b) and (c) corresponding to $SmFe_8Mo$, $SmFe_8V$ and $SmFe_8Ti$, respectively. The fracture surface of $SmFe_8Ti$ ribbons in Fig. 9(c) particularly shows considerably fine grains under 5000 Å which primarily is responsible for the high coercivity of the $SmFe_8Ti$ and $SmFe_{7.8}Ti_{0.8}$ compounds. Intrinsic magnetic properties of single phased Fe_3Mo were measured to clear the role of Fe_3Mo. The exhibited coercivity values were 200 ~ 340 Oe, and the observed saturated moment was

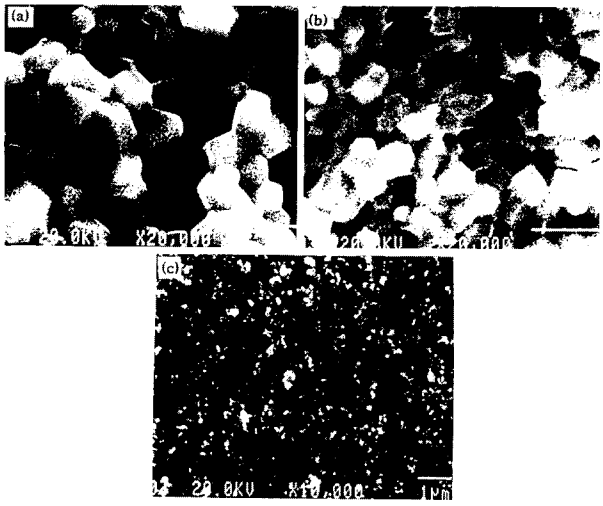

Fig. 9. SEM micrographs showing the grain aspect at fracture surface of (a) $SmFe_8Mo$, (b) $SmFe_8V$ and (c) $SmFe_8Ti$ ribbons, respectively.

2.4 ~ 3.4 kG. This value of coercivity is almost the same to that of α-Fe which is magnetically soft. Accordingly the enhancement in coercivity of $SmFe_8M$ compounds could be attributed to the fine size of $Sm(Fe, M)_7$ grains, where the exact reason for grain refinment could not be clarified yet. Since the formation of Fe_3M and α-Fe articles was not confirmed to taek place along the grain boundary, one of the possible explanation for the enhanced coercivity may be based on the random anisotropy model of microcrystalline magnetism[15] which is well explained for melt-spun $Sm(Fe_{11}Ti)$ ribbons of $ThMn_{12}$ structure. It gives the correct magnitude of coercivity varying as the reciprocal of the crystallite size[15]. As a reference the characteristics of typical phases of previously reported Sm-Fe pseudo binary compounds are summarized in Table I.

Table I. Characteristics of typical Sm-Fe systems prepared by rapid solidification

alloy composition	process	phase identified	lalttice parameter (Å)		Curie temp.(℃)	crystal structure	Ref.
			a	c			
$Sm_{12}Fe_{88}$	melt-spun ribbon	Sm_2Fe_{17}	4.936	4.147	117	rhomb.	(11)
$Sm_{10}Fe_{90}$	-	$SmFe_7$	4.877	4.289	200	rhomb.	(11)
$Sm_{15}Fe_{70}V_{15}$	mechanical alloying	$Sm(Fe,V)_{12}$	8.563	4.802	310	tetragonal.	(6)
$SmFe_{10}Ti$	sputtering	$Sm_5(Fe,Ti)_{17}$	20.12	12.34	305	hexa.	(9)
$SmFe_8M$ (M=Mo,V,Ti)	melt-spun ribbon	$Sm(Fe,M)_7$	4.891	4.20	355	rhomb.	present work

The alloys with Sm contents more than 10 at.%, i. e., $Sm_{12}Fe_{88}$ and $Sm_{15}Fe_{70}V_{15}$ were always found to form in Sm_2Fe_{17} and $Sm(Fe, V)_{12}$ structures, respectively, with the presence of $SmFe_2$ Laves phase, while the pseudo binary $SmFe_{10}Ti$ and the present $SmFe_8M$(M = Mo, V, Ti) stoichiometry crystallized in single phased $Sm_5(Fe, Ti)_{17}$ and $Sm(Fe, M)_7$, respectively. The formation of minor α-Fe in the $SmFe_8M$ compounds was confirmed to take place as fine particles in the $Sm(Fe, M)_7$ matrix as shown in Fig. 10. Fig. 10(a) is a TEM micrograph showing the $Sm(Fe, Mo)_7$ grains and (b) is electron diffraction pattern obtained from (a). The inset in (a) is an electron microdiffraction pattern obtained from the α-Fe particle indicated by an open arrow. The $Sm(Fe, Mo)_2$ phase is also can be seen around the $Sm(Fe, Mo)_7$ grains indicated by dark arrows. As Cadieu et al.[9] claimed, the additives M do not go to the grain boundaries but would be substitutionally solutionized in the matrix phase. In Fig. 11 we have plotted the

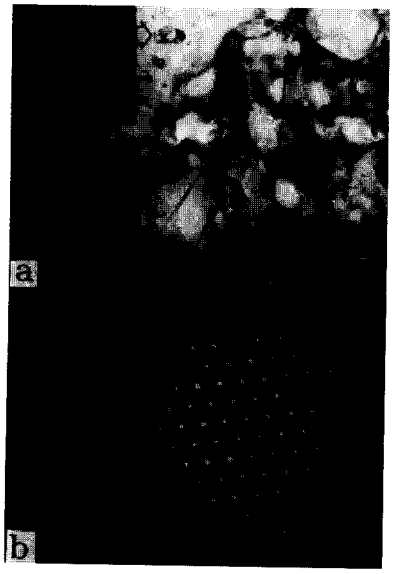

Fig. 10. (a) TEM micrograph showing the $Sm(Fe, Mo)_7$ grains, and (b) is a electron diffraction pattern obtained from (a). The inset in (a) is a microdiffraction pattern obtained from the Fe_3Mo particle indicated by an arrow.

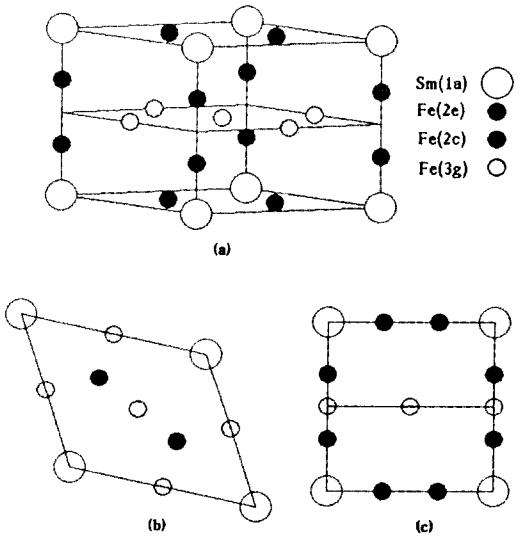

Fig. 11. Crystal structure of the $Sm(Fe, M)_7$ phase group P6/mmm.

the structure of $Sm(Fe, M)_7$ phase belong to the space group P6/mmm, where (c) is the plot viewing right side of (a).

Ⅳ. Conclusion

New hard magnetic phase based on $Sm(Fe, M)_7$ (M = Mo, V, and Ti) crystal structure was found to form in rapidly solidified $SmFe_{7+x}M_x$ compound. The $Sm(Fe, M)_7$ crystals of the space group P6/mmm with a = 4.891 and c = 4.20 Å exhibit strong coercive force such as ${}_iH_c = 3 \sim 6$ kOe to have an energy product, $(B.H)_{max} = 4.5 \sim 5.0$ MGOe. Such a magnetically hard properties indicate a strong potential for a commercial use. In this paper we reported the existance of $Sm(Fe, M)_7$ phase for the first time in Sm-Fe binary system.

References

[1] A. Muller, J. Appl. Phys., **64**(1988) 249.

[2] D. B. deMooij and K. H. J. Buschow, J. Less-Common Metals, **136**(1988) 207.

[3] J. Hu, T. Wang, S. Zhang and Z. Wang, J. Magn. Magn. Mater., **74**(1988) 22.

[4] G. Schneider, F. J. G. Landgraf, V. Villas-Boas, F. P. Missell and A. E. Ray, Materials Letters, **8**(1989) 472.

[5] N. Kamprath, N. C. Liu, H. Hedge and F. J. Cadieu, J. Appl. Phys., **64**(1988) 5720.

[6] K. Schnitzke, L. Schultz, J. Wecker and M. Katter, Appl. Phys. Lett., **56**(1990) 587.

[7] M. Katter, J. Wecker and L. Schultz, Appl. Phys. Lett., **56**(1990) 1377.

[8] H. H. Stadelmier, G. Schneider, E. T. Henig and M. Ellner, Materials Letters, **10**(1991) 303.

[9] F. J. Cadieu, H. Hedge, R. Rani and K. Chen, Materials Letters, **11**(1991) 284.

[10] K. H. J. Buschow in : ed. E. P. Wohlfarth, Ferromagnetic Materials vol. **4**, North-Holland, Amsterdam(1988) pp. 44 ~ 46.

[11] K. H. J. Buschow and A. S. van der Goot, Acta Cryst., **B27**(1971) 1085.

[12] M. Katter, J. Wecker and L. Schultz, J. Appl. Phys., **70**(6)(1991) 3188.

[13] C. J. Yang, W. Y. Lee and S. D. Choi, J. Magn. Magn. Mater., **114**(1992) 18.

[14] C. J. Yang, W. Y. Lee and S. D. Choi, Materials Letters., **12**(1991) 233.

[15] H. Sun, Y. Otani and J. M. D. Coey, J. Appl. Phys., **67**(9)(1990) 4659.

급속냉각된 $SmFe_{7+x}M_x$ 화합물에서 생성된 신 강자성상

朴彦柄 · 崔承德 · 楊忠軫

산업과학기술연구소, 전자기소재연구실, *P.O.Box 135, 790-600* 포항시

(1994년 6월 12일 받음, 1994년 9월 13일 최종수정본 받음)

철-희토류 화합물인 Sm-Fe 이원계에서 조성식 $SmFe_{7+x}M_x$(M = Mo, V, Ti) 화합물을 급속냉각기술로 제조하여 강자성을 나타내는 새로운 자성상인 $Sm(Fe, M)_7$을 합성하였다. Sm-Fe 이원계에 제 2의 천이원소 Mo, V 또는 Ti를 첨가함으로써, $Sm(Fe, V)_7$ 자성상은 큐리온도(Tc)가 355 ℃에 달했으며 x = 0.8 과 1.0 사이에서 $SmFe_{7+x}M_x$(M = Mo, V, Ti)의 고유보자력($_iH_c$)이 3 ~ 6 kOe를 갖는 신 자성상을 제조하였다. $Sm(Fe, M)_7$ 상은 급냉응고 된 상태에서나 열처리 후에도 변함없이 안정하였으며 오히려 급냉상태에서 보다 우수한 강자기 특성을 보였다. $Sm(Fe, M)_7$은 육방정계 결정구조를 갖는 능방정계이며 P6/mmm Space Group 에 속하는 것으로 판명되었다. $Sm(Fe, M)_7$ 자성상이 고보자력을 나타내는 원천적인 이유는 급속냉각에 의하여 결정입도가 2000 ~8000 Å의 미립자로 형성되기 때문이며, 높은 큐리온도를 보이는 까닭은 급속냉각에 의해 제 2의 천이원소인 Mo, V 또는 Ti의 Fe에 대한 고용도가 평형상태에서 보다 월등히 높아져 자기변환온도를 상승하게 하였기 때문이다.